JMEPEG (2004) 13:129-134
DOI: 10.1361/10599490418307

1059-9495/$19.00

Effect of Chemical Composition Variation on Microstructure and Mechanical Properties of a 6060 Aluminum Alloy

M.S. Silva, C. Barbosa, O. Acselrad, and L.C. Pereira

(Submitted 23 January 2003; in revised form 12 January 2004)

The 6XXX series aluminum alloys (Al-Mg-Si) are widely used in many different engineering and architectural applications. These alloys usually undergo a thermal treatment, which consists of a heat treatment solution and artificial aging, since the desirable mechanical properties depend on the microstructural state of the material. The recycling of materials has been increasing recently for economic and ecologic reasons. By using scrap as raw material, important reductions in energy and total costs can be achieved, and, at the same time, negative environmental impacts can be greatly reduced. In the present work, the possibility of using a larger amount of scrap as raw material in the production of an AA 6060 alloy is evaluated by analyzing the difference in microstructure and mechanical properties between a commercial 6060 alloy and a variation with higher Fe and lower Si contents that was specially produced for this study. Both materials were placed into a heat treatment solution at 560 °C for 1 h, and then underwent water quenching followed by artificial aging at 180 °C for different periods of time. Hardness and tension tests were used to evaluate the mechanical properties. Light and transmission electron microscopy have been used to determine important features such as grain size before and after being placed into the heat treatment solution, and the characteristics of the second-phase particles in the two materials. This study leads to the conclusion that a higher amount of scrap material can be used in the production of 6060 Al alloy without significant changes in mechanical properties compared with the more usual compositions.

Keywords aluminum alloys, mechanical properties, microstructure, recycling, thermal treatment

1. Introduction

The 6XXX series aluminum (Al) alloys are extensively used in extrusion processes due to their excellent workability. The performance of these alloys during the extrusion process as well as the properties of the final product are strongly dependent on the microstructural state of the material.

The AA 6060 alloy has chemical composition limits that are well defined by the ASTM standards. Within these limits, the major part of the industrial production concentrates on a higher silicon (Si) and lower iron (Fe) and chromium (Cr) range, which will be considered as the standard 6060 alloy in this work. However, there is an increasing demand from the industrial sector for using large amounts of scrap material in the production process to reduce fabrication costs. This implies an increase in the content of Fe and Cr in the final composition of the 6060 alloy. Therefore, another batch of Al was cast with higher contents of Fe (as an impurity) and Cr and lower contents of Si, but still within the conventional limits of the 6060 alloy. In this study, this alloy will be identified as the 6060-A alloy. The disadvantage of the high Fe content is the enhanced probability of forming large particles of AlFeSi,[1-4] an intermetallic phase that can lower the workability of the alloy. On the other hand, Si has an important role together with magnesium (Mg) in forming Mg_2Si, or β phase, the intermediate species of which, β″, is the main hardening precipitate in the alloy.[5-8] Cr may assist in the formation of the AlFeCrSi phase, which has a very important role in the grain size control.[9-11]

In the second half of the 20th century, the recycling of used products (i.e., scrap material) gained increased importance due to its economic and ecologic advantages. Today, there are the expressions "primary metal production," which refers to the production of metals using ingots as raw material, and "secondary metal production," which refers to the production of metals using scrap as raw material. Al alloys are supposed to be one of the most easily recycled materials, at least compared with other important industrial materials like steels and polymers. Recently, in Europe, North America, and Japan, laws controlling the use of scrap as a raw material in the fabrication of new products have been introduced.[12]

The most important cases of Al recycling are in the automotive industry and in the food and beverage packing industry. In the case of the automotive industry, there is a strict requirement for high purity levels in the scrap to be used as raw material. This fact makes the classification of scrap an important step in the whole recycling process. In fact, the growth of recycling is strongly dependent on the development of an efficient framework for collecting, classifying, separating, and handling scrap material. Light alloys, such as Al alloys, can be easily separated from ferrous alloys by gravimetric processes. The Al scrap from vehicles can have high contents of Fe and Si, but, even in these cases, the Al can be used in the fabrication of low-value components or as a complement in a

M.S. Silva, C. Barbosa, O. Acselrad, and **L.C. Pereira,** COPPE, Federal University of Rio de Janeiro, P.O. Box 68505, CEP 21.945-970, Rio de Janeiro, Brazil. Contact e-mail: cassiob@int.gov.br.

wide composition of different raw materials. Another important issue is the fusion loss of scrap, a loss of 10% on average compared with 1% from primary raw materials such as ingots. However, even considering these losses, the cost of scrap is so much lower than the cost of the primary raw Al that a considerable profit is realized with its use (25% or more), not to mention the reduction in electrical energy consumption, which is even more significant. Based on all of these reasons, one can say that Al recycling has a great future.[12]

The aim of this work was to analyze the effects of using a larger amount of scrap in the production of the 6060 alloy, and, as a consequence, to study the influence of the chemical composition variation on the microstructural features and mechanical properties. With this purpose in mind, hardness and tensile tests, as well as light and transmission electron microscopy (TEM) techniques were used to determine the characteristics of both materials (i.e., 6060 and 6060-A alloys) before and after being placed in a heat treatment solution followed by aging at 180 °C for different periods of time.

2. Materials and Methods

The 6060 and 6060-A alloys were received as extruded bars supplied by Almax Alumínio Ltd. (Rio de Janeiro, Brazil). The chemical composition ranges are shown in Table 1. The

Table 1 Composition of the Alloys (wt.%)

Alloy	Mg	Si	Fe	Cu	Mn	Cr	Zn	Ti	Al
6060	0.405	0.549	0.176	0.040	0.064	0.007	0.022	0.022	Bal. (a)
6060-A	0.400	0.405	0.239	0.067	0.062	0.015	0.046	0.030	Bal.

(a) Bal., balanced

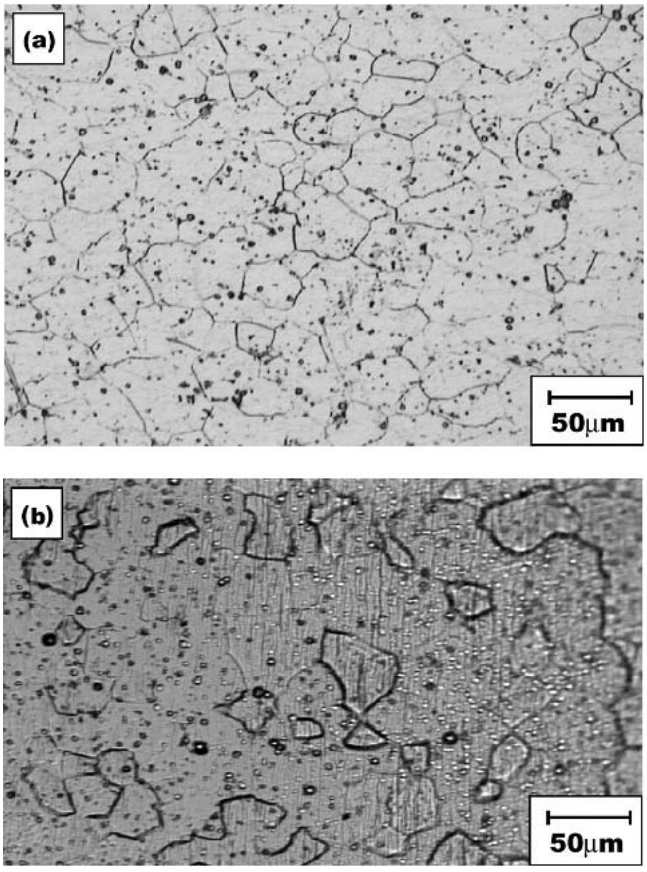

Fig. 1 Alloy 6060-A: as-received **(a)** and SHT **(b)** (from optical microscopy)

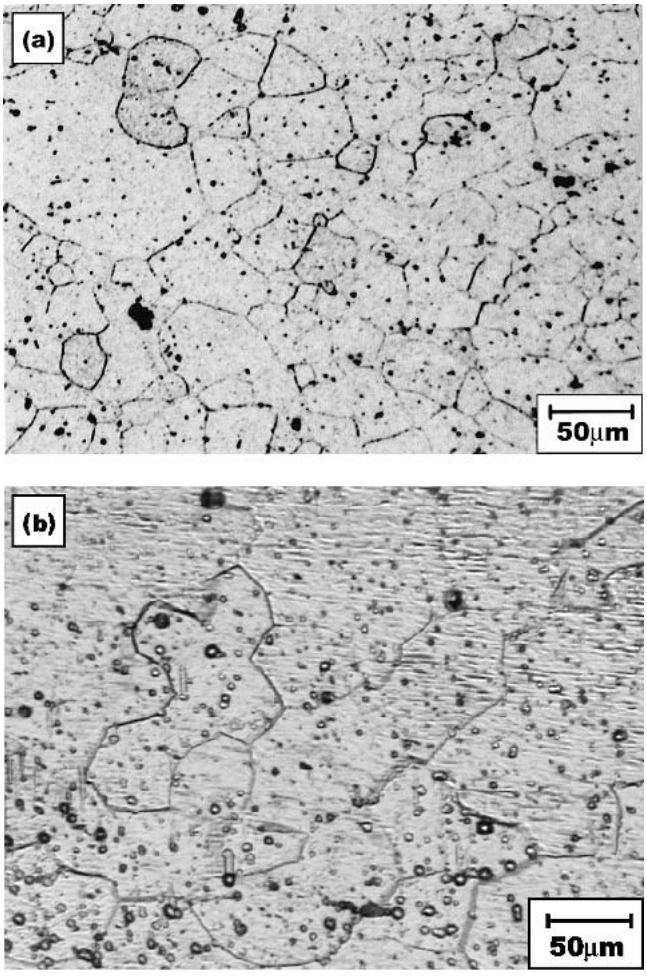

Fig. 2 Alloy 6060: as-received **(a)** and SHT **(b)** (from optical microscopy)

amounts of Fe and Cr in the 6060-A alloy were pushed closer to the upper limits of the ASTM standard for the 6060 alloy, whereas the Si content was lower than the amount usually recommended for conventional applications. The samples were given T6 processing, as follows: heat treatment in a solution at 560 °C for 1 h, followed by water quenching, and then artificial aging at 180 °C for 2, 4, 6, 8, 10, and 12 h. Brinell hardness (HB) tests were performed on samples in the as-received, solution heat treated (SHT) and SHT + aged conditions. For each sample, an average hardness value was calculated as well as the standard error, which enabled the determination of the error bars for a confidence level of 95%. Equations 1 and 2 were used to determine the standard error (S) and the statistical parameter δ:

$$S = [\Sigma (X_i - X_n)/(n-1)]^{1/2} \quad \text{(Eq 1)}$$

$$\delta = t \cdot S/(n)^{1/2} \quad \text{(Eq 2)}$$

In these equations, n is the number of measurements for each sample, and t is the Student's parameter (which is 2 for the 95% confidence level).

Nine tensile test samples were prepared according to the E-8 ASTM standard for each alloy. For tensile testing, only three conditions were chosen: samples aged for 4, 6, and 8 h. Three tests were performed for each condition, and the same statistical procedure was used to evaluate the tensile properties, which included ultimate tensile strength (UTS), yield strength (YS) and total elongation (ε).

Samples for optical microscopy underwent the standard procedure of grinding on 100, 220, 400, 600, and 1200 mesh SiC papers, followed by 3 μm alumina and then 1 μm diamond paste polishing. The samples were etched in a 4% NaOH solution for 3 min followed by an immersion in a 5% HNO_3 solution.

The samples for TEM analysis were obtained as 3 mm diameter discs, which had been ground to about 90 μm thickness and then electrolytically polished in a 30% HNO_3-70% ethanol solution using a Tenupol (Struers, Ballerup, Denmark) twin jet polishing unit operating at 12 V and 0.15 A for about 3 min. The images were obtained in a CM20 microscope (Phillips, Amsterdam, The Netherlands) operating at 200 kV. The TEM was equipped with for x-ray energy dispersive spectroscopy (EDS) and x-ray mapping for qualitative chemical analysis.

Table 2 Effect of the Solution Heat Treatment on the Grain Size

Alloy	Condition	Grain Size, μm	
		Longitudinal	Transverse
6060	As received	34.8	32.8
	SHT	60.5	49.2
6060-A	As received	43.2	28.4
	SHT	56.8	56.6

3. Results

The grain structures of both the 6060 and 6060-A alloys are shown in Fig. 1 and 2, in the as-received (extruded) condition and after heat treatment in solution. The measured grain sizes are shown in Table 2. The original as-received grain sizes are quite comparable, but the results in Table 2 show clearly that subsequent grain growth due to immersion in the heat treatment solution is faster for the 6060-A alloy. The SHT grain structure in the case of the 6060 alloy is practically twice as large as the initial one, whereas for the 6060-A alloy it grew by a factor of nearly three.

Figures 3 and 4 show the evolution of the mechanical properties of the alloys during the aging treatment, up to a maximum aging time of 12 h. The values for yield stress (YS) and ultimate tensile stress (UTS) at 4, 6, and 8 h are stated in Table 3, together with the relative variation $\Delta_{i,j}$ of each property within the 4-6 and 6-8 h time intervals. $\Delta_{i,j}$ is defined as $(X_j - X_i)/X_i$, where X_n is the value of the property X at the aging time $t = n$.

Fine precipitates in the heat-treated alloys are shown in TEM images in Fig. 5-8. AlFeCrSi particles (shown in Fig. 5)

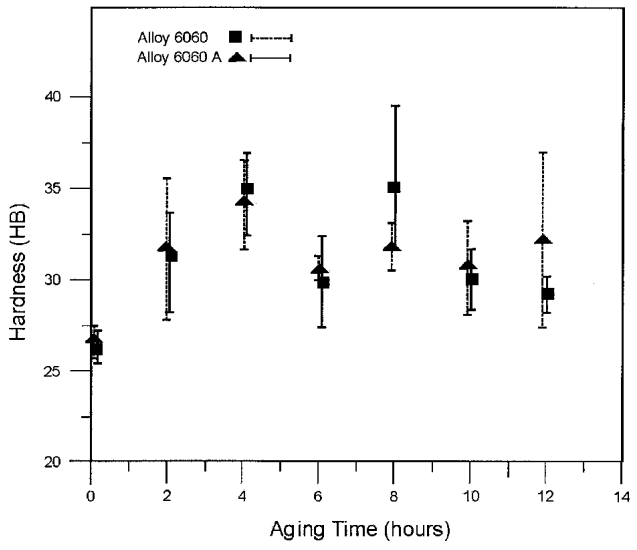

Fig. 3 Hardness evolution during aging

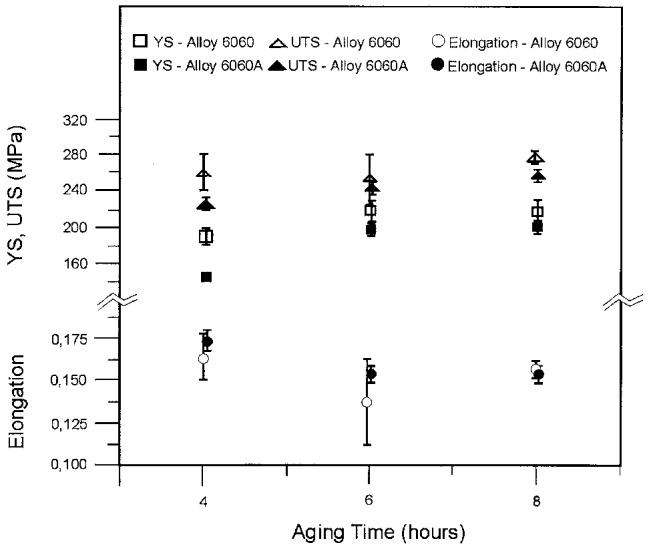

Fig. 4 Mechanical properties evolution during aging

were only seen in the 6060-A alloy, which has the higher Cr content. The EDS spectrum is shown in Fig. 6. AlFeSi precipitates like the one shown in Fig. 7 have been detected in both alloys. β″ needles (Fig. 8) appeared in both alloys after complete aging.

4. Discussion

4.1 Microstructural Aspects

Both alloys exhibit, after undergoing identical extrusion processing, grain sizes on the order of 30-40 μm (Fig. 1,2). During the solution heat treatment, moderate grain growth has occurred for both alloy compositions, leading to similar final grain structures, as seen in Fig. 1 and 2, and expressed numerically in Table 2.

The alloys are quite similar in terms of other microstructural details. The only significant difference noted between them is the presence of dispersoids of the AlFeCrSi kind (Fig. 5), which were observed only in the 6060-A alloy and were almost certainly due to its higher Cr content. The composition was revealed by the EDS spectrum (Fig. 6). Other particles, such as AlFeSi (Fig. 7), which were identified by x-ray mapping for chemical analysis, were detected in both alloys as well as in the β″ needles, which appear after 8 h of artificial aging (Fig. 8).

4.2 Mechanical Properties

The analysis of the hardness and tensile tests presented in Fig. 3 and 4 show that higher Fe content and lower Si content give results very close to the ones presented by the standard material (6060). After 8 h of aging, there is a superposition of the hardness values of both materials. The hardness curve shows a small variation between 4 and 8 h for both alloys. However, the evolution of the YS, and mainly the one for the UTS, shows that the aging process is complete after 8 h. The main differences between the two alloys were found during aging. Table 3 shows the YS and UTS values for the different aging times, and the $\Delta_{i,j}$ values give an idea of the evolution of the aging kinetics in each time interval.

It can be seen that the aging kinetics values are higher for the 6060-A alloy, and are significantly higher between 4 and 6 h of aging. The YS increase in the 6060-A alloy within such a time interval is about twice the one for the 6060 alloy, and in both alloys the increase in the following time interval is much lower at less than 5%. A possible explanation could be the higher content of solute elements in the 6060-A alloy, which is about 20% higher than in the 6060 alloy. During the initial

Table 3 Evolution of YS and UTS Values During Aging

	YS, MPa					UTS, MPa				
Alloy	4h	6h	8h	$\Delta_{4,6}$	$\Delta_{6,8}$	4h	6h	8h	$\Delta_{4,6}$	$\Delta_{6,8}$
6060	188	224	226	0.19	0	263	262	280	0	0.07
6060-A	140	195	206	0.39	0.05	216	247	259	0.14	0.05

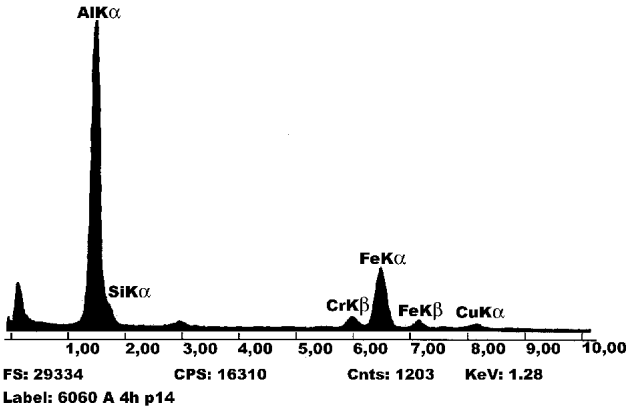

Fig. 6 EDS spectrum in AlFeCrSi particle

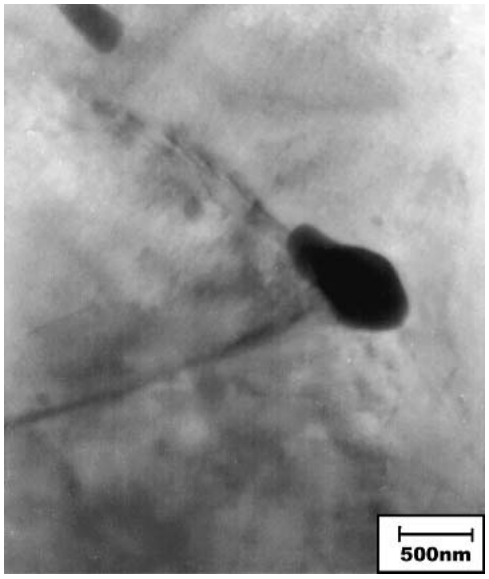

Fig. 5 AlFeCrSi particle in alloy 6060-A (by TEM)

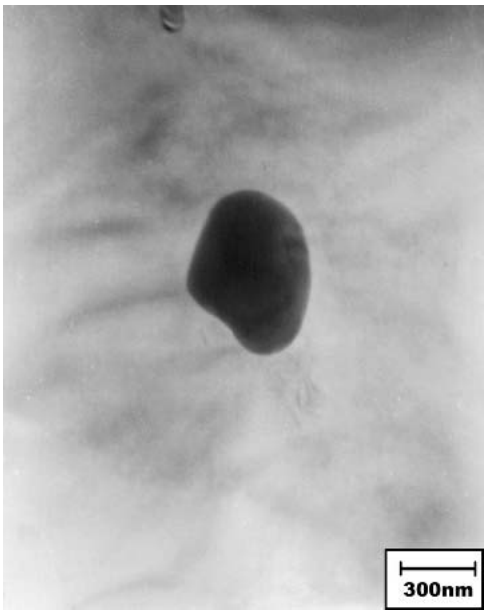

Fig. 7 AlFeSi particle in alloy 6060 (by TEM)

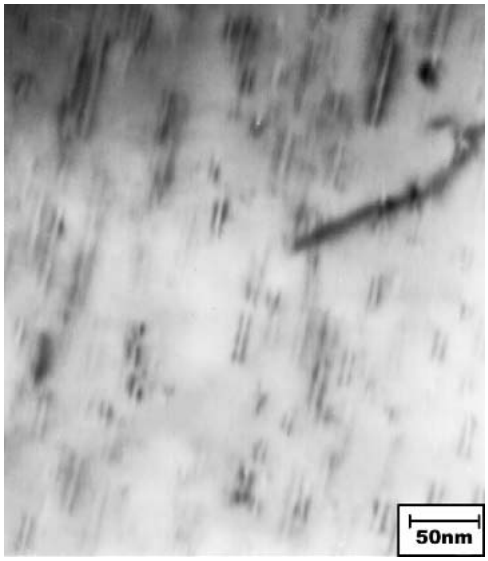

Fig. 8 β″ precipitates in alloy 6060 artificially aged (8 h at 180 °C)

stages of aging, atomic movements toward the constitution of Guinier-Preston zones are accelerated in the 6060-A alloy to reduce elastic distortions in the Al matrix, and this movement may even overcome the possible retarding effect due to the slower diffusion of Si atoms resulting from the higher content of other solute atoms. The very close strength values for each alloy after 8 h of aging, despite the difference in Si content, can be explained by the formation of dispersoid particles still during the SHT, which are very stable at the aging temperatures.[9-11]

Despite the higher Fe content of the 6060-A alloy, the ductile behavior of both alloys is very similar. The presence of Fe can help in the formation of β-AlFeSi and α-AlFeCrSi particles at the grain boundaries, which could lower the ductility of this alloy, but this has not been detected in the current study. The lower Si content in turn leads to the formation of a smaller amount of hardenable precipitates, which has a beneficial effect on ductility.[5-8]

The elongation values are almost identical, and, regarding strength, the variation for the 6060-A alloy shows UTS and YS to be only 10% lower (20 MPa). Therefore, one comes to the conclusion that the use of a material with a higher amount of scrap as a starting raw material does not have any significant detrimental effect on mechanical properties. In the same way, there is no difference in the behavior of the 6060-A alloy during the extrusion process when compared with the 6060 alloy, based on comparative observations during industrial extrusion processing of the two alloy versions. The final conclusion is that a higher content of Fe and Cr and a lower content of Si, which may result from a larger use of scrap metal during the fabrication of AA 6060 alloys, does not affect the final mechanical properties required for the different applications of this alloy.

5. Conclusions

The possibility of producing a 6060 Al alloy with a higher Fe content, which would enable the use of a larger amount of scrap in the production of this alloy, was analyzed in this work. With this purpose in mind, mechanical testing results and a microstructural characterization of the standard 6060 alloy were compared with the material produced with higher Fe and Cr content and lower Si content. This analysis led to the conclusion that the mechanical performance of both alloys after an aging treatment at 180 °C for 8 h is very similar, with differences in UTS, YS, and elongation values being less than 10%.

The possibility of negative effects on ductility due to the presence of particles on the grain boundaries seems to be compensated for by the smaller amount of hardenable precipitates that also contain Si. It was also found that a significant difference in the aging kinetics occurred in each alloy. This seems to be faster in the case of the 6060-A alloy and is probably due to the higher amount of solute elements, which increase the driving force for the nucleation of precipitates during the initial stages of the precipitation process.

TEM results provide important evidence of the relevance of artificial aging on the formation of hardenable precipitates and of the presence of Cr-rich particles in the 6060-A alloy, which were not seen in the standard 6060 alloy.

Based on these results, one can say that, from a mechanical performance point of view, there is no serious restriction to the use of higher Fe content than the ones usually adopted for the standard 6060 alloy. This means that a higher amount of scrap material can be used in the production of 6060 Al alloy.

Acknowledgments

The authors wish to thank Mr. M.P.S. Borgerth and Almax Alumínio Ltd. for supplying the alloys used in the present work and for providing operational facilities, Research Center of Petrobrás (Brazilian Oil Company) (CENPES)/Petrobrás and Université Libre de Bruxelles for allowing the use of research facilities, and Brazilian Agency for Educational Support (CAPES), Brazilian Agency for Research Support (CNPq), Agency for Research Support from Rio de Janeiro State (FAPERJ), and University Foundation José Bonifácio (FUJB) for financial support.

References

1. S. Murali, K.S. Raman, and S. Murthy: "Morphological Studies on β-FeSiAl$_5$ Phase in Al-7Si-0.3 Mg Alloy with Trace Additions of Be, Mn, Cr and Co," *Mater. Charact.*, 1994, *33*, p. 99-112.
2. S. Murali, K.S. Raman, and S. Murthy: "Effect of Magnesium, Iron (impurity) and Solidification Rates on the Fracture Toughness of Al-7Si-0.3Mg Casting Alloy." *Mater. Sci. Eng.*, 1992, *A151*, pp. 1-10.
3. G. Gustafsson, T. Thorvaldsson, and G.L. Dunlop: "The Influence of Fe and Cr on the Microstructure of Cast Al-Si-Mg Alloys," *Metall. Trans. A*, 1986, *17A*, pp. 45-52.
4. L.O. Gullman, S. Zajac, A. Johansson: "The Influence of Small Mn Additions and Heat Treatment Practice on the Extrudability of AA 6005 Aluminum Alloy" in *Proc. 5th International Aluminum Extrusion Technology Seminar, II,* May 19-22, The Aluminum Association, Washington, DC, 1992, pp. 71-77.
5. G.A. Edwards, K. Stiller, G.L. Dunlop, and M.J. Couper: "The Precipitation Sequence in Al-Mg-Si Alloys," *Acta Mater.*, 1998, *46*(11), pp. 3893-904.
6. N. Maruyama, R. Uemori, N. Hashimoto, M. Saga, and M. Kikuchi: "Effect of Silicon Addition on the Composition and Structure of Fine-Scale Precipitates in Al-Mg-Si Alloys," *Scripta Mater.*, 1997, *36*(1), pp. 89-93.
7. W.H.V. Geertruyden and W.Z. Misiolek: "Thermal Cycle Simulation

of 6xxx Aluminum Alloy Extrusion" in *Proc. 7th International Aluminum Extrusion Technology Seminar, II*, May 16-19, The Aluminum Association, Washington, DC, 2000, pp. 381-86.
8. J.E. Hatch: "Aluminum: Properties and Physical Metallurgy," ASM, Metals Park, OH, 1990, pp. 139-45.
9. L. Lodgaard and N. Ryum: "Precipitation of Dispersoids Containing Mn and/or Cr in Al-Mg-Si Alloys," *Mater. Sci. Eng. A*, 2000, *A283*, pp. 144-52.
10. R.C. Dorward and C. Bouvier: "A Rationalization of Factors Affecting Strength, Ductility and Toughness of AA 6061-Type Al-Mg-Si-(Cu) Alloys," *Mater. Sci. Eng. A*, 1998, *A254*, pp. 33-44.
11. G. Scharf and B. Grzemba: "Notch Sensitivity in Wrought AlMgSi Alloys" in Proc. 3rd International Aluminum Extrusion Technology Seminar, May 15-18, The Aluminum Association, Washington, DC, 1984, pp. 47-52.
12. D. Altenpohl: *Aluminium von Innen*, Aluminium-Verlag, Düsseldorf, 1994, pp. 398-99 (in German).